UU Master's Thesis

Universiteit Utrecht

Reconstructing millennial scale temperature and precipitation variability in monsoonal East Asia during MIS3 using branched tetraether membrane lipids

Shivam Mishra[1], Kirsten de Haan[1], Jingjing Guo[1], Louise Fuchs[1], Youbin Sun[2], Francien Peterse[1]

1 Department of Earth Sciences, Utrecht University, the Netherlands

2 Institute of Earth Environment, Chinese Academy of Sciences, Xi'an, China

6511384

Course code: GEO4-1520

ECTs: 45

Contents

Abstract

Monsoons are seasonal changes in wind direction and associated precipitation driven by land-sea temperature contrasts. The East Asian monsoon is among the largest systems on Earth, and its history is mainly derived from oxygen isotope ($\delta^{18}O$) records of cave stalagmites and loess-paleosol sequences from the Chinese Loess Plateau (CLP). However, these records represent a mixed signal of both temperature and precipitation, which hampers assessing the response of monsoon precipitation to ongoing global warming. To create independent records for temperature and precipitation for East Asia, we here use branched glycerol dialkyl glycerol tetraethers (brGDGTs), a suite of membrane-spanning lipids synthesized by soil bacteria that record changes in temperature and (precipitation-induced) soil pH in their molecular structure stored in the Yuanbao section located on the western edge of the CLP. The high sedimentation rate in this section allows us to focus on millennial scale climate variations that occurred during Marine Isotope Stage – 3 (MIS3, spanning from 27 to 55 ka BP). Our high-resolution temperature record indeed shows millennial scale variability, although decoupled in timing from the magnetic susceptibility and grain size records for this same section that instead follow the global-scale variations that characterize MIS3. This decoupling suggests that the brGDGT-derived temperatures likely reflect a more local signal. This was attributed to glaciation trends on Tibetan plateau which maximize during the early MIS3. In addition, the strong influence of the westerlies at Yuanbao makes it prone to changes in the Atlantic Ocean circulation. Creating similar multi-proxy records across the CLP should reveal the extend of local temperature conditions on the CLP and its influence on East Asian monsoon dynamics.

1.Introduction

A monsoon is the seasonal change in wind direction driven by land-sea temperature contrasts leading to wet or dry periods. The East Asian Monsoon (EAM) system is characterized by a winter monsoon, with dominating winds from the cold-core Siberia-Mongolia High, and a summer monsoon, during which winds bring warm and moist air masses from the South China Sea and the Bay of Bengal (Lu and Chan 1999) (Fig. 1).
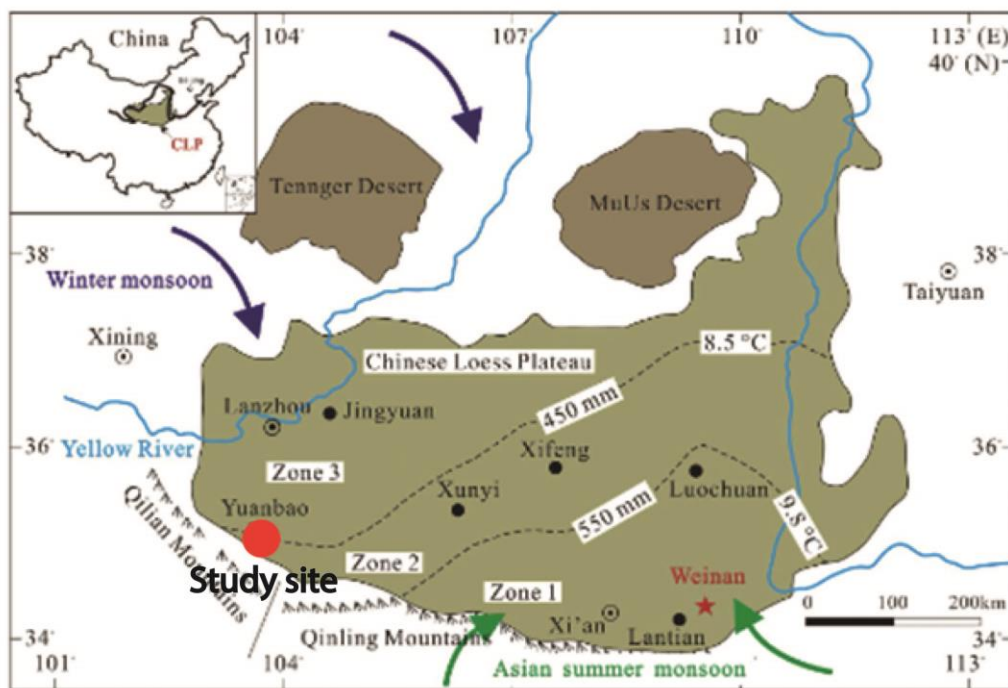
Figure 1. The map shows the Chinese Loess Plateau (CLP) indicating some of the key locations, referred to in the text. Yuanbao (red), the section sampled in this thesis is located on the western edge.

These seasonal winds and the associated precipitation are not only an integral component of global climatic systems but also a lifeline for the economics and people of East Asia (An et al., 2000). Thus, the stability and variability of the East Asian Monsoon are of wide concern, especially because of the potential for the monsoon to change with global warming. This makes analyzing of relevant paleoclimatic

records crucial to understand the response of this monsoon system to modern global warming. Paleoclimatic records become relevant as our contemporary, instrumental records are not long enough.

Traditionally, our understanding of past monsoonal climate evolution is derived from marine sediment records, using various proxies. Proxies are physical and/or chemical characteristics, derived from the geological sequence that represent certain environmental or climatic conditions. Marine records are relatively contiguous (in time) and can be studied with proxies such as benthic $\delta^{18}O$ values (Lisiecki, 2005). Marine records integrate a larger area and hence represent a more global climatic record. Climate archives with a similar resolution and continuity are scarce on the terrestrial realm. The Chinese Loess Plateau (CLP) is considered as one of the best locations to study Quaternary climate variability on land, specifically as an archive of East Asian Monsoon climate variability. These deposits are characterized by aeolian deposits and provide a robust and contiguous record, which goes back to 22 million years (Guo et al., 2002; Rao et al., 2013). The Pleistocene sections are characterized by silty loess deposits that alternate with paleosols (Porter and An, 1995). It is assumed that the loess layers are deposited during cool and dry periods and the paleosol layers are formed during warm and moist periods and can be linked to the glacial-interglacial cycles also recognized in paleoclimate reconstructions from the global benthic stack (Porter and An, 1995). During glacial periods, a larger grain size fraction is deposited as the loess-carrying westerlies are strengthened and deposition is rate is higher. During interglacials, the loess deposition rate is lower as a result of the warmer and wetter climate, which also facilitates soil formation. The resulting alternation of loess and paleosols layers are reflected by magnetic susceptibility.

The climatic changes recorded on the CLP are also recorded by the $\delta^{18}O$ values of cave stalagmites in China (Wang et al., 2001). Despite the congruence of these data sets, both the loess and the stalagmite records represent a mixed signal of temperature and precipitation, due to the fact that monsoonal precipitation and temperature are positively correlating, and both soil formation as well as the oxygen isotopic composition of precipitation do not only depend on precipitation, but also on temperature. This hampers our understanding of the influence of warming on EAM precipitation. Hence, in order to

understand the response of warming on monsoon precipitation, we need methods to separate these two parameters, by creating independent, yet directly comparable records for temperature and precipitation.

In this thesis project, branched glycerol dialkyl glycerol tetraethers (brGDGTs), which are membrane-spanning lipids presumably synthesized by heterotrophic soil bacteria (Weijers et al., 2006), are used to generate a continuous, absolute, high resolution temperature record for continental East Asia. The brGDGTs contain 4–6 methyl branches (Fig. 2), the number of which has an empirical relationship with air temperature (Weijers et al., 2007). Based on the occurrence of brGDGTs in a global collection of modern soils, it was shown that temperature (approximated by mean annual air temperature; MAAT) can be estimated based on the Methylation of Branched Tetraethers (MBT), where the number of methyl branches increases with decreasing temperature. Furthermore, the abundance of cyclopentane moieties in branched GDGTs relates to soil pH and serves as a proxy for pH. Soil pH can used as a proxy for precipitation. (Weijers et al., 2007).

After the improvement in the chromatography methods, the brGDGTs with a methyl group located at C-6 instead of the C-5 position of the alkyl chain was discovered, where the relative amount of 6-methyl brGDGTs appeared to relate to soil pH. Separation of 6-methyl brGDGTs from the 5-methyl brGDGTs in the global soil calibration data set has allowed to remove the pH – dependence from the MBT index (proxy for temperature), which was then adjusted to include only 5 -methyl isomers in the MBT'5me index, creating a pure temperature proxy (De Jonge et al., 2014). Simultaneously, a 6-methly based function capturing the isomerization of branched tetraethers (IBT) was formulated as a pH proxy (Xiao et al., 2015). Subsequently, the global soil dataset was expanded to derive a new function to transfer MBT'5me index values into mean air temperatures using a Bayesian approach (Dearing Crampton-Flood et al., 2020).
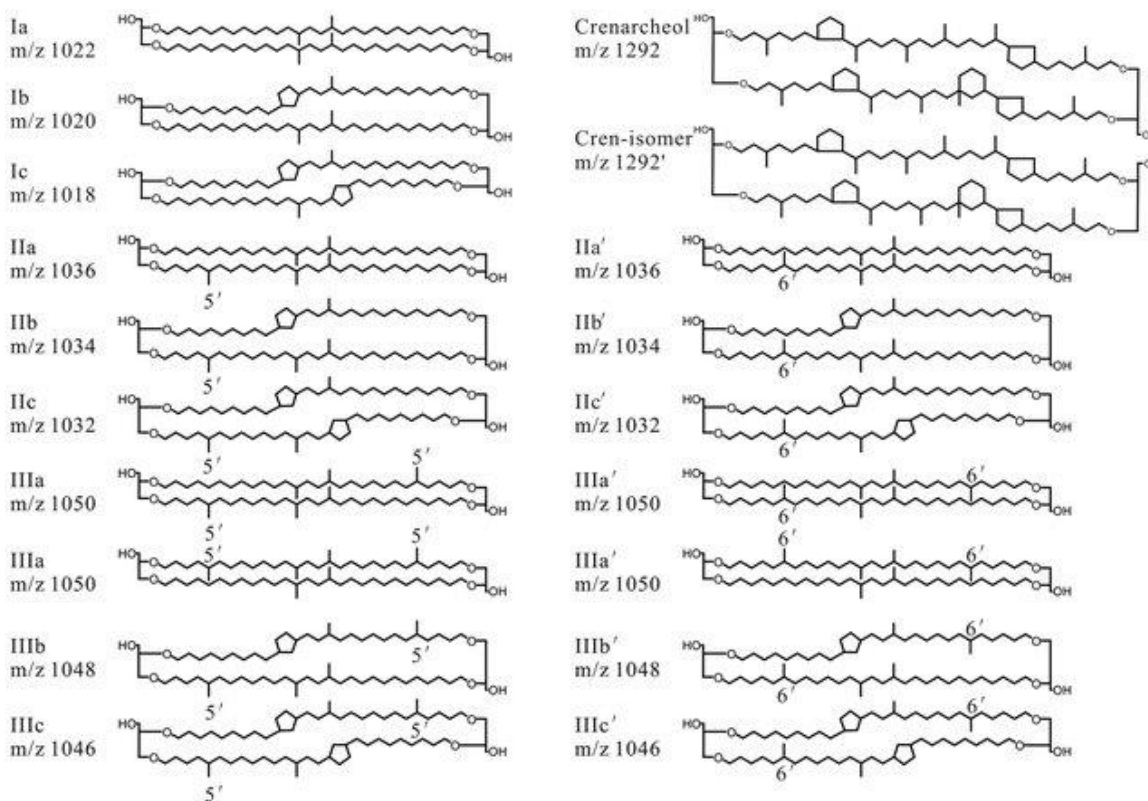
Figure 2. Chemical structures of branched GDGTs (I-III) and crenarchaeol (IV) (Wang et al, 2018).

This thesis will focus on creating separate records of temperature and precipitation-induced changes in soil pH using brGDGTs stored in a loess section at Yuanbao (Fig. 1). The records will be created for Marine Isotope Stage 3 (MIS 3) – a period between 60 and 27 ka ago during the last glacial cycle, where climate was known to be highly variable. MIS3 is also a relatively warmer period between the glacial periods of MIS4 and MIS2 as seen in Figure 3, where the insolation is high and stable between 60ka – 27 ka. Global climatic records like the Greenland ice core data and the speleothem data from the Hulu and Sanbao caves display relatively high millennial scale variability during this period. Investigating if and how these millennial scale climatic variations are recorded on the CLP is the primary objective of the study.
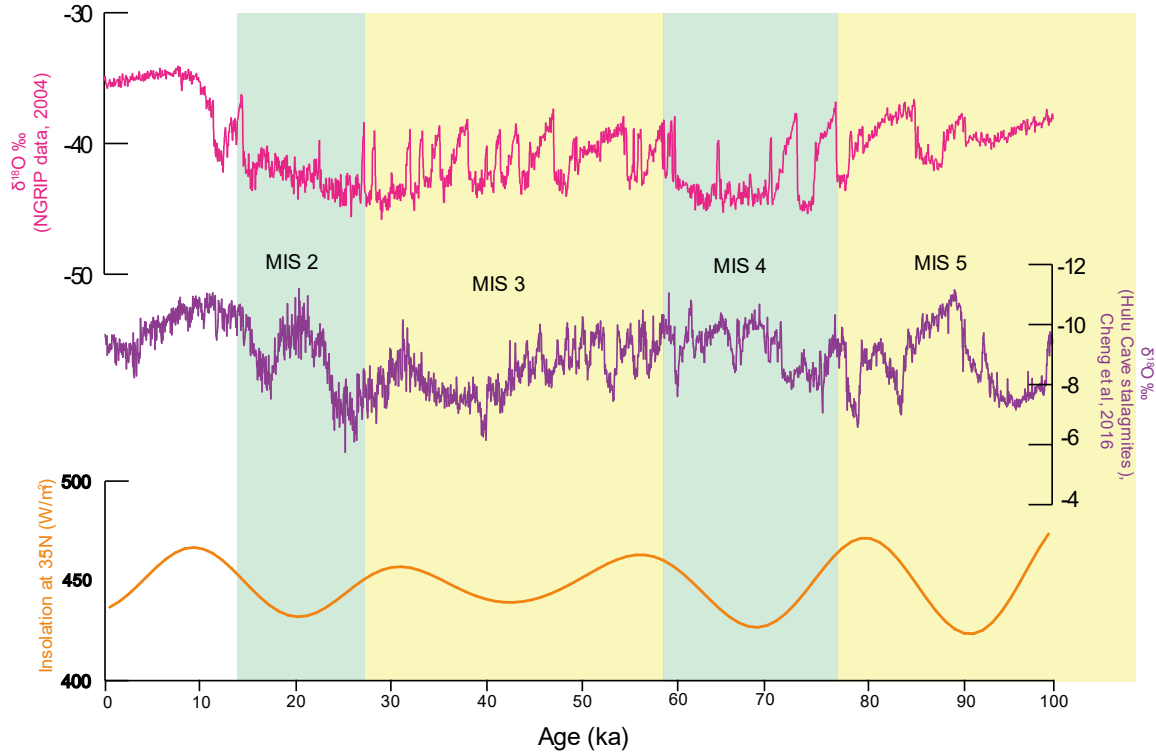
Figure 3. Top to bottom: NGRIP data, δ¹⁸O records, 100 ka b.p. (NGRIP, 2004). Hulu cave data δ¹⁸O from speleothems, complied by Cheng et al., 2016. Variability of insolation at 35N (recorded in June) over the last 100 thousand years.

Yuanbao, our study site, is located on boundary of the monsoon-dominated East Asia and westerlies-dominated Central Asia. Hence, we expect our records to integrate both monsoonal and westerly signals (Li, 1990; Herzschuh, 2006). This makes the signal at Yuanbao particularly important when trying to understand temperature and precipitation changes across the CLP.

Furthermore, it is the furthest section on the CLP from the ocean and the closest section to the source of the loess, which causes high sedimentation rates at Yuanbao. This gives us an opportunity to reconstruct continuous, high-resolution temperature and precipitation records. The section also lies adjacent to the Tibetan Plateau (TP), on the foothills of the Qilian mountains, which form the eastern margin of the TP as seen in Fig. 1.

2.Method

2.1. Study Site and Sampling

Yuanbao (35°38′45.7″N, 103°09′04.8″E) is located on the western edge of the CLP (near Linxia city) at an altitude of 2177 m a.s.l. (Lai et al., 2007). The mean annual temperature at Linxia is around 7 °C, with winter temperature below freezing. The precipitation at the site is concentrated in the summer months (April – August), accounting for 80% of the annual precipitation (Jia et al., 2013). The Qilian mountains form the eastern edge of the Tibetan Plateau in Fig. 1 and Yuanbao is located on the eastern, windward side of these mountains. Due to its location close to the source area of the loess (Tennger Dessert), the Yuanbao section is characterized by high sedimentation rates, making it an ideal site for high resolution climate reconstruction (Guo et al., 2021). The section was samples at 5 cm resolution in summer 2019 and based on the OSL dates of Lai et al., (2007), grain size and magnetic susceptibility records, the interval between 15 to 23m (intended to cover MIS3) was targeted for brGDGT analyses.

2.2. Extraction and Analysis

After freeze-drying, samples number 830 to 2115 were ground and homogenized. BrGDGTs were extracted from 30g loess of each depth, with a mixture of dichloromethane (DCM) and MeOH (9:1, v/v) in a MEX microwave at 70°C. The obtained total lipid extract (TLE) was filtered over a filter paper (Whatman grade 42.55 mm diameter). 99ng of GDGT standard was added to each sample and they were dried under a gentle nitrogen stream. The TLEs were separated into an apolar and a polar fraction using an activated Al_2O_3 column and eluting with hexane:DCM (9:1) and DCM:MeOH (1:1), respectively. The polar fraction which contains the brGDGTs was analyzed by ultra-high-performance liquid chromatography-mass spectrometry (UHPLC-MS) with settings according to Hopmans et al. (2016). By scanning the $[M+H]^+$ ions (protonated mass) in selected ion monitoring (SIM) mode, the target

compounds were detected at *m/z* 1050 (brGDGT–IIIa), 1048 (brGDGT–IIIb), 1046 (brGDGT–IIIc), 1036 (brGDGT–IIa), 1034 (brGDGT–IIb), 1032 (brGDGT–IIc), 1022 (brGDGT–Ia), 1020 (brGDGT–Ib), 1018 (brGDGT–Ic), with *m/z* 744 for the internal standard. Quantitation was achieved by peak area integration of the [M+H]$^+$ ions in Chemstation software B.04.03.

2.3 brGDGT-based index calculations

BrGDGT distributions was translated to temperature estimates using the MBT'5me index (De Jong et al., 2014, Equation 1) and globally-calibrated transfer functions of Naafs et al (2017) and Dearing Crampton-Flood et al (2020). The pH was calculated using IBT using Eq. 2 and the IBT was converted into pH using Eq. 3 (Xiao et al, 2015).

$$\text{MBT'}_{5ME} = (Ia + Ib + Ic)/(Ia + Ib + Ic + IIa + IIb + IIc + IIIa) - \text{Eq. 1}$$

$$\text{IBT} = -\log \frac{\text{IIa}' + \text{IIIa}'}{\text{IIa} + \text{IIIa}} - \text{Eq. 2}$$

$$\text{pH} = 6.53 - 1.55 \times \text{IBT} - \text{Eq. 3}$$

3.Results

3.1. Climatic signals recorded by brGDGTs in Yuanbao

The brGDGT- derived temperature and pH records were plotted along with loess proxies (magnetic susceptibility (MS) and grain size (GS)) from the same loess section, along with $\delta^{18}O$ values of speleothems from the Hulu/Sanbao cave, precession, and the GRIP record (Figure 4). The loess proxy records show an inverse relation with the speleothem $\delta^{18}O$ record. This is evident by the fact that peaks of the MS record align with the troughs of the speleothem record which is plotted on an inverse axis to show the inverse relationship. This implies that for the speleothem, $\delta^{18}O$ values are lower during interglacial periods and vice-versa.

Air temperature ranges from ~11 °C to ~2 °C between 67 ka to 32 ka. Soil pH ranges from 7.1 to 6.4 in the same time period. A higher pH represents that the evapotranspiration is higher than the precipitation. Therefore, pH here is a proxy for monsoonal intensity (in relation to evaporation) which is controlled by both temperature and precipitation. The brGDGT-derived records, i.e., air temperature and pH are not coherent with the loess and global proxies.

From 44 ka to 33 ka, pH is synchronous with major trends of the GS and MS records. The temperature during this time period shows relatively higher variability, ranging from 11 to 4 °C. The pH and temperature records are also synchronous. This period is shaded with pink in Fig 4. On the contrary, the mid-MIS3 period, from 56 ka to 45 ka, shows no coherence, not just between the two brGDGT-derived records but also with those of the loess proxies. During this period, the pH signals still react to precipitation but temperature remains low and stable, only varying within 2 – 3 degrees. From 60 ka to 45 ka there is a clear decrease in temperature coupled with a relatively large variability in MS. This period is shaded with blue in Fig. 3. Furthermore, the pH during this time period still shows a relatively higher variability to that of temperature, ranging from the higher pH values in the record, to one the lowest

values recorded. Hence the record is divided into a non-synchronous period (blue) and a synchronous

period (pink).
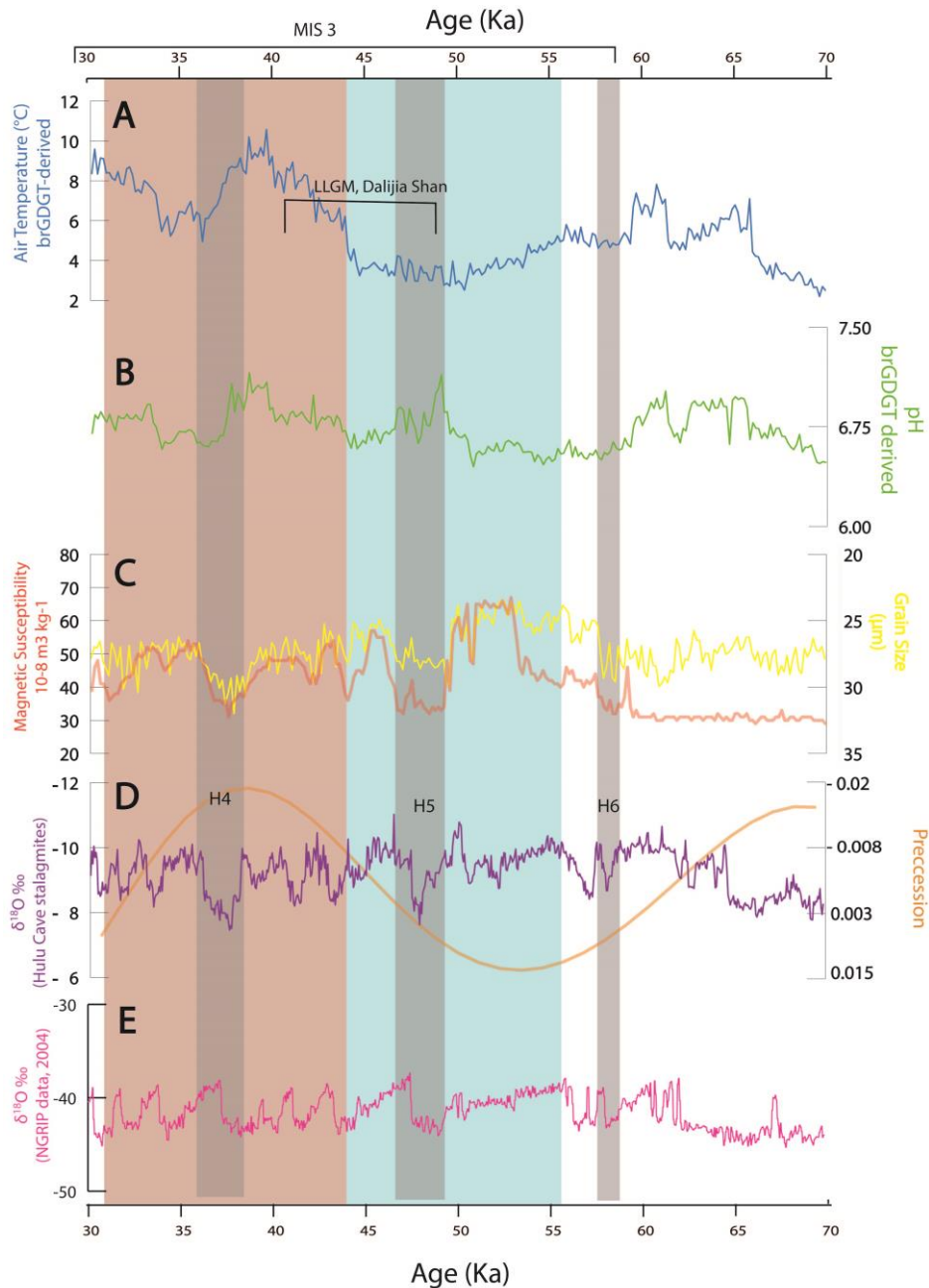
Figure 4. Records of A) brGDGT-based average air temperatures (for months above freezing), B) brGDGT-derived soil pH indicating monsoon precipitation intensity, C) magnetic susceptibility and grain size for the Yuanbao sequence, D) Hulu cave δ18O (Wang et al., 2001) and precession. H4, H5 and H6 represent the Heinrich events, calibrated by comparing with GRIP data. E) Greenland ice core record δ18O, (GRIP, 2004). last glacial local maximum at at Dalijia Shan on the Tibetan Plateau (Wang et al., 2015). Pink shaded segment: The brGDGT-based records display synchronous trends with other proxies and with themselves. Blue shaded segment: The derived records display non-synchronous trends with other proxies and with themselves.

4. Discussion

4.1 Global vs local climate signals at Yuanbao

The temperature record based on brGDGTs is non-coherent with the MS and GS records (Fig. 4). Though the degree of coherence of the trends changes over time, demarcated by the blue and pink shaded segments in Fig. 4. The first inference that can be made is that the brGDGT-derived records do not represent global climatic changes. Being one of the few records, based on location-specific terrestrial proxies, it is possible that the brGDGT-derived records represent a more local climatic regime that manifested at Yuanbao during the MIS3. This local climatic record could be a combination of several factors, including global climatic events and local geographical features. Hence, the blue and pink shaded segments possibly represent two different climatic forcings on the site.

4.2 The influence of Tibetan Plateau on the climate at Yuanbao

The most significant geographical feature in the vicinity of Yuanbao is the Tibetan Plateau (TP). The plateau itself is one of the major features on the Earth's lithosphere and exerts influence on the global climatic cycle. It exhibits unique localized climatic features due to high mean altitude and sheer size (Hahn and Manabe, 1975; Yanai et al., 1992). Furthermore, the TP and the related orogen display distinct patterns with regards to precipitation and glaciation. Tibet and High-mountain Asia (HMA) host unique accumulation and ablation regimes due to the monsoonal control on the climate in this part of the world (Shi, 2002).

In Europe and North America, summer is the glacial ablation season and winter is the accumulation season. In the Asian-monsoonal context, summer becomes both the ablation and accumulation season, where the strength of the monsoonal-precipitation has a strong control on the expansion and reduction of glaciers on the Plateau (Fujita and Ageta, 2000). The extent of glaciers in this region would probably have an influence on the temperature in the near vicinity and the foothill regions. Since our section lies close

foothills of the eastern Tibetan mountains, it can be hypothesized that glacial dynamics on these mountains could have influenced the climate in and around Yuanbao.

The Die Shan (34º15´ to 34º19´N, 102º56´ to 103º14´E) and Dalijia Shan (35˚240 –35˚380 N, 102˚290 – 102˚320 E) are mountains located on the north-east border of the Tibetan Plateau. Dalijia Shan is around 60 km east of the section and Die Shan is bit closer, around 50 km south of section (Fig. 5).
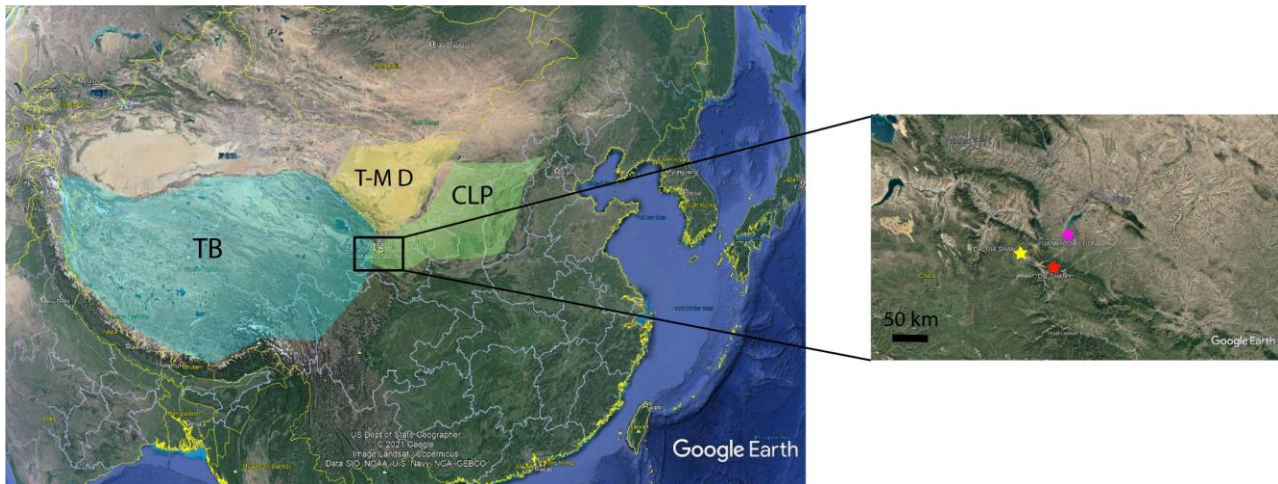
Figure 5 – Map showing the Tibetan Plateau (TB), the Tengger-Mu Us Dessert and Chinese Loess Plateau (CLP), in relation to our section. <u>Inset</u>: Pink (Yuanbao section), Yellow (Dalijia Shan) and Red (Die Shan).

Wang et al. (2015) and Cui et al (2018) focus on Dalijia Shan and Die Shan respectively. The studies have reconstructed the Equilibrium Line Altitude (ELA), to assess the glacial extent on the mountains during the MIS3 and MIS2 periods. The Dalijia Shan study used a precipitation-temperature model and the Die Shan study used an Energy and Mass Balance model to determine paleo-temperature in the MIS3 in relation to the glaciation. Despite the geographic and methodical differences in the studies, both studies concluded that the maximum extent of glaciation on both mountains was during the Mid-MIS3, and not during the global Last Glacial Maximum in the MIS2, which would be expected. This Local Last Glacial Maximum hypothesized by the studies, extends from around 51 ka to 41 ka, the temperature depression marked as 'Mid-MIS3' in Fig.6
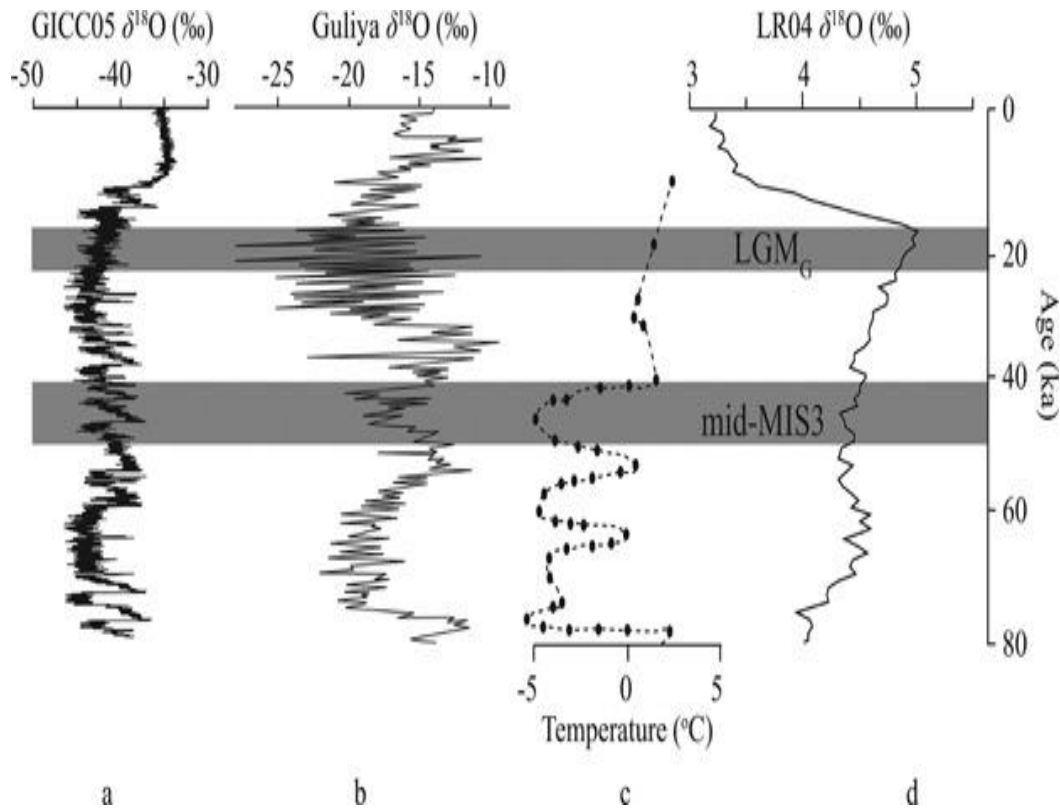
Figure 6. Figure taken from Wang et al., 2015. a – Greenland ice core $\delta^{18}O$ (Wolff *et al*., 2010). b – Guliya ice core $\delta^{18}O$ (western Tibet; Yao *et al*., 1997). c – Core from Zioge basin (eastern Tibet plateau; Wu *et al*., 2000).d – Global benthic $\delta^{18}O$ stack. (Lisiecki and Raymo, 2005).

Figure 6 displays four temperature records derived from different proxies. Record 'b' and record 'c' are derived from sites in and around the Tibetan plateau. The Guliya ice-core (b) is located on the western side of the TP and the Zoige basin (c) is located on the eastern edge of the TP like Yuanbao. These two records display the temperature depression which corresponds to the temperature depression in the brGDGT- derived record, as marked in Figure 4. Records 'a' and 'd' display global climatic records derived from the Greenland ice core and the global benthic stack respectively. The two global records do not display a clear decrease in temperature around the same time i.e., between 50 ka and 40 ka. Therefore, it can be inferred that the low temperatures at this time are induced by a local climatic forcing possibly related to the Tibetan plateau.

Another study, by Heyman et al. (2011), has also sampled the NE Tibetan Plateau (Bayan Har Shan) and used [10]Be exposure ages from boulder and sediment samples to reconstruct glacial advances and has concluded that the most recent glacial maximum on Bayan Har Shan has occurred at the minimum age of 65-40 ka, well within the MIS3, and not the erstwhile assumed MIS2 glacial maximum.

The plausible theory for these observations could be the overall strengthening of solar insolation during the MIS3 (Prell and Kutzbach, 1987), also seen in Fig. 4 and Fig. 3. The stronger insolation would induce higher terrestrial temperatures; hence the monsoons would be strengthened throughout this period, despite some internal fluctuations. There is a slight decrease in insolation around 50 -45 ka. The coupling of an overall high monsoonal perception with a slight decrease in in temperature could promote glaciation. Moreover, the Eastern part of the plateau would experience a relatively stronger influence of the summer monsoon (compared to central and western Tibet) and receive higher precipitation being on the monsoonal windward side of the Tibetan plateau. This could result in a precipitation-driven accumulation, dominating the temperature-controlled ablation. The expansion of glacial and ice peaks would cool the mountains and also the foothills of those mountains on the eastern Tibetan edge, where the Yuanbao section is located. This would imply a very localized, relatively cold and wet pocket during the mid MIS3 in that region. There are possible other factors that lead to an expansion of glaciers during this time in the MIS3 which could be influenced by the extent of the westerlies and the cold climate that associated with them.

4.3 Yuanbao records in global context

Yuanbao is located at the edge of the monsoonal extent, which is a 'transitional zone' between 'Westerlies dominated Asia' and 'Monsoonal dominated Asia' (Caves et al., 2015, Fig. 1). It is also plausible that the influence of these two circulation systems changes with time in response to global climatic events and the glacial cycles. The other sections sampled on the CLP are well within the monsoonal regime hence Yuanbao possibly displays a unique mixed westerly-monsoonal signal, which

should be recorded by the pH record. Soil pH is used as a proxy for precipitation, as mentioned earlier. If the precipitation is higher during a given period of time, the record is expected to display a lower pH, given that evaporation is not the controlling factor (Slessarev et al., 2016). The main source of precipitation and the dominant season of precipitation could be changing over time. This implies that for the Yuanbao section, at given periods of time westerlies could have been a major control on the pH record.

One of the major millennial scale controls on the westerlies is the Atlantic Meridional overturning circulation (AMOC) (Li et al., 2019). Abrupt variations in the AMOC, during the MIS3 have been cited as one of the reasons for millennial scale variability which is characteristic of this time period (Clement and Peterson 2008; Sun et al. 2012). A robust AMOC is associated with a higher freshwater forcing that results in a decrease in latitudinal temperature gradient. This is attributed to warming of the midlatitudes by a stronger heat transfer towards the Arctic. A lowered contrast in pressures between the mid-latitudes and central Asia weakens the Westerlies and the velocity of the winds (Sun et al., 2011). It can be inferred that the Westerlies were displaying sharp changes in the strength and extent of precipitation as they are closely linked to the AMOC. It is therefore possible that climatic changes in the Atlantic have an influence on the reach of Westerlies in Asia, and, therefore, indirectly influence Yuanbao at given periods of time.

Henry et al. (2016) used radio isotope ratios of ^{231}Pa/^{230}Th from foraminifera in Bermuda rise sediments as a proxy for lateral transport. The ^{231}Pa/^{230}Th ratio of the foraminifera in North Atlantic sediments is used as a proxy for lateral transport. Weaker lateral transport is associated with strengthening of the Westerlies resulting from a weak AMOC. When comparing the ^{231}Pa/^{230}Th ratio with the temperature record from Yuanbao (Fig. 7), it can be observed that, during what is defined as the temperature depression in the temperature record, there is a relative increase in ^{231}Pa/^{230}Th, which would indicate relatively stronger Westerlies (marked with a pink line in Fig. 7). As seen in Fig 4, the increase in soil pH indicates drier conditions during H4. This period aligns with an increase in GS, further supporting the

claim of stronger westerlies. This could be explained as a period where the dominant climatic forcing is

the westerlies, where the boundaries of the area influenced by westerlies would have shifted further east.

A time period where the air temperature is displaying limited variability, as it remains low and stable, this

temperature depression is further aided due to local influences like the expansion of Tibetan glaciers.

Only precipitation record (pH) displays relative variability. This phenomenon also coincides with a rising

precession (decreasing insolation) during this time.
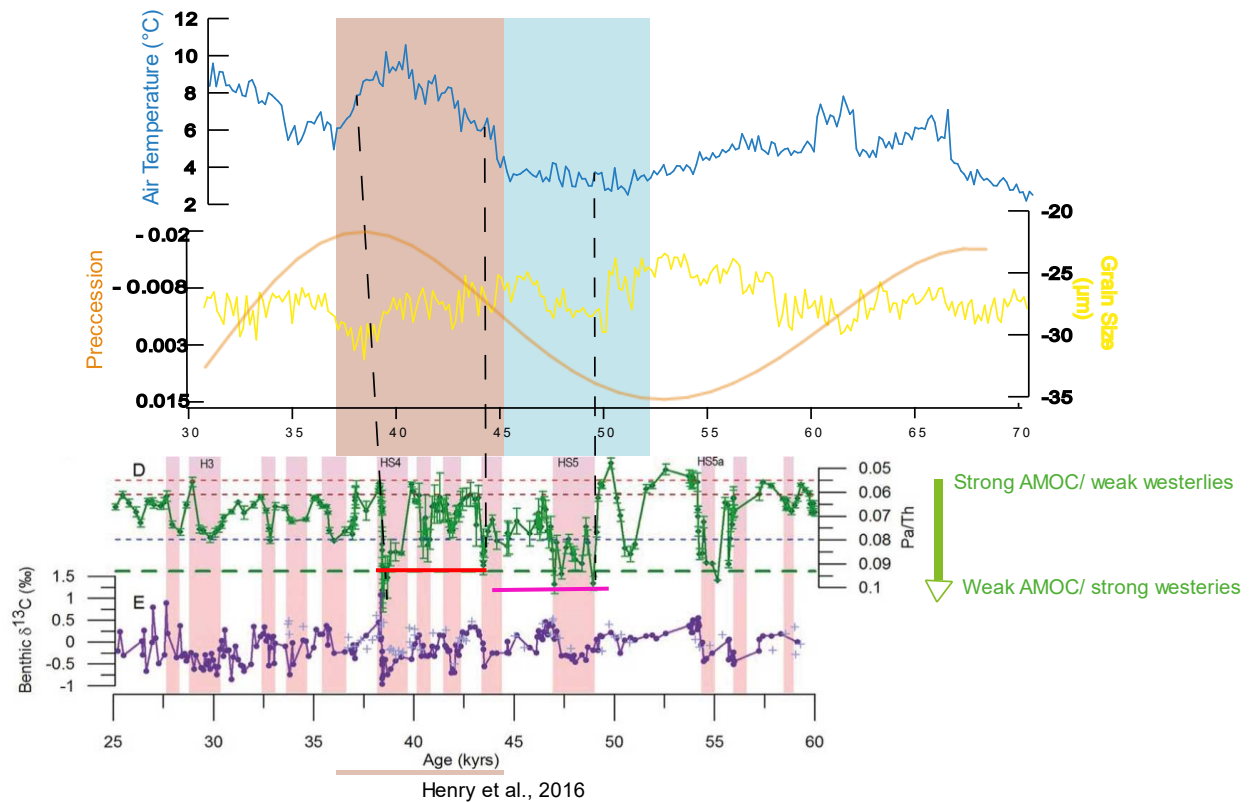
Figure 7. Air Temperature (GDGT-derived) record, precession and grain size, plotted with the Pa/Th record from Henry et al., 2016. A relatively high phase of Pa/Th (marked with pink line) aligns temporally with the temperature depression and a relative low phase (marked with red line) in the Pa/Th signal aligns with the increase in temperature.

The time interval from 43ka to 32ka (shaded by the pink in Figs. 4 and 7) coincides with a low Pa/Th

signal (the upper limit marked by red in Fig 7.). This would mean that the maximum strength of the

westerlies would decrease, marked by a relative receding of westerlies dominated Asia. This is evident by

the relative GS decrease as the GS record enters from blue shaded period to pink shaded period. This can

be interpreted as a return of a monsoonal climate. During this time, the pH and temperature records are

synchronous. It can be inferred that the soil pH could be temperature controlled, i.e., driven by temperature-induced evapotranspiration. The relative rise in temperature and return to a monsoonal climate could be explained by the heightened insolation and the receding of glaciers in Eastern Tibet. Therefore, the blue-shaded time period represents a westerlies and glacier influenced period where Yuanbao experiences a colder climate. The pink shaded region is warmer period where the summer monsoon is the dominant climatic forcing.

5.Conclusions

The application of brGDGT-based proxies (i.e., MBT'5me and IBT) for temperature and soil pH to the loess-paleosol sequence at Yuanbao has resulted in continuous, high-resolution records displaying clear millennial scale climate characteristics of the MIS3 interval. Interestingly, the trend in temperature and precipitation do not align with loess proxy records representing global climate processes. This discrepancy can be explained if the temperature and precipitation signals reflected by the brGDGT proxies are interpreted as a more local climate signal, likely resulting from the position of Yuanbao in relation to the Tibetan Plateau. The colder than expected temperatures recorded by the air temperature record could result from larger than expected glacial expansion on the TP.

In addition, the western location of the Yuanbao makes it more sensitive to influences of the westerlies, in comparison to other sections in the CLP. The westerlies appear to be strengthened from 50 ka to 43 ka, owing to changes in the AMOC. A combination of local and global climatic factors led to the temperature depression during the first half of MIS3. The decoupling between local and global climatic processes can be identified by comparing different proxies as seen for Yuanbao. Similar multi-proxy records for other sections (along the E-W transect of CLP) would provide further insight into the influence of different climatic factors on the CLP. The relative influence of westerlies and the summer monsoon, and the influence of topography like the Tibetan plateau and other mountain ranges could delineated through such multiproxy records.

References

An, Z., Kukla, G. J., Porter, S. C., & Xiao, J. (1991). Magnetic susceptibility evidence of monsoon variation on the Loess Plateau of central China during the last 130,000 years. Quaternary Research, 36(1), 29-36.

Caves, J. K., Winnick, M. J., Graham, S. A., Sjostrom, D. J., Mulch, A., & Chamberlain, C. P. (2015). Role of the westerlies in Central Asia climate over the Cenozoic. Earth and Planetary Science Letters, 428, 3hCui, H., Wang, J., Yu, B., Hu, Z., Yao, P., & Harbor, J. M. (2018). Marine Isotope Stage 3 paleotemperature inferred from reconstructing the Die Shan ice cap, northeastern Tibetan Plateau. Quaternary Research, 89(2), 494.

De Jonge, C., Hopmans, E. C., Zell, C. I., Kim, J. H., Schouten, S., & Sinninghe Damsté, J. S. (2014). Occurrence and abundance of 6-methyl branched glycerol dialkyl glycerol tetraethers in soils: Implications for palaeoclimate reconstruction. Geochimica et Cosmochimica Acta, 141, 97-112.

De Jonge, C., Stadnitskaia, A., Hopmans, E. C., Cherkashov, G., Fedotov, A., & Sinninghe Damsté, J. S. (2014). In situ produced branched glycerol dialkyl glycerol tetraethers in suspended particulate matter from the Yenisei River, Eastern Siberia. Geochimica et Cosmochimica Acta, 125, 476-491.

Crampton-Flood, E. D., Tierney, J. E., Peterse, F., Kirkels, F. M., & Damsté, J. S. S. (2020). BayMBT: A Bayesian calibration model for branched glycerol dialkyl glycerol tetraethers in soils and peats. *Geochimica et Cosmochimica Acta*, *268*, 142-159.

Fujita, K., & Ageta, Y. (2000). Effect of summer accumulation on glacier mass balance on the Tibetan Plateau revealed by mass-balance model. Journal of Glaciology, 46(153), 244-252.

Guo, Z. T., William F. Ruddiman, Q. Zetal Hao, H. B. Wu, Y. S. Qiao, Ri X. Zhu, S. Z. Peng, J. J. Wei, B. Y. Yuan, and T. S. Liu. "Onset of Asian desertification by 22 Myr ago inferred from loess deposits in China." Nature 416, no. 6877 (2002): 159-163.

Hahn, D. G., & Manabe, S. (1975). The role of mountains in the south Asian monsoon circulation. Journal of Atmospheric Sciences, 32(8), 1515-1541.

Henry, L. G., McManus, J. F., Curry, W. B., Roberts, N. L., Piotrowski, A. M., & Keigwin, L. D. (2016). North Atlantic ocean circulation and abrupt climate change during the last glaciation. Science, 353(6298), 470-474.

Herzschuh, U. (2006). Palaeo-moisture evolution in monsoonal Central Asia during the last 50,000 years. Quaternary Science Reviews, 25(1-2), 163-178.

Heyman, Jakob, Arjen P. Stroeven, Marc W. Caffee, Clas Hättestrand, Jonathan M. Harbor, Yingkui Li, Helena Alexanderson, Liping Zhou, and Alun Hubbard. "Palaeoglaciology of Bayan Har Shan, NE Tibetan Plateau: exposure ages reveal a missing LGM expansion." Quaternary Science Reviews 30, no. 15-16 (2011): 1988-2001.

Lai, Z., Wintle, A. G., & Thomas, D. S. (2007). Rates of dust deposition between 50 ka and 20 ka revealed by OSL dating at Yuanbao on the Chinese Loess Plateau. Palaeogeography, Palaeoclimatology, Palaeoecology, 248(3-4), 431-439.

Li, Y., Song, Y., Yin, Q. et al. Orbital and millennial northern mid-latitude westerlies over the last glacial period. Clim Dyn **53,** 3315–3324 (2019).

Lisiecki, L. E., & Raymo, M. E. (2005). Pliocene-Pleistocene stack of globally distributed benthic stable oxygen isotope records, PANGAEA.

Peterse, F., Martínez-García, A., Zhou, B., Beets, C. J., Prins, M. A., Zheng, H., & Eglinton, T. I. (2014). Molecular records of continental air temperature and monsoon precipitation variability in East Asia spanning the past 130,000 years. Quaternary Science Reviews, 83, 76-82.

Porter, S. C., & Zhisheng, A. (1995). Correlation between climate events in the North Atlantic and China during the last glaciation. Nature, 375(6529), 305-308.

Prell, W.L., Kutzbach, J.E., 1987. Monsoon variability over the past 150000 years. Journal of Geophysical Research 92, 8411–8425.

Rao, Z., Chen, F., Cheng, H., Liu, W., Lai, Z., & Bloemendal, J. (2013). High-resolution summer precipitation variations in the western Chinese Loess Plateau during the last glacial. Scientific Reports, 3, 2785.

Shi, Y. (2002). Characteristics of late Quaternary monsoonal glaciation on the Tibetan Plateau and in East Asia. Quaternary International, 97, 79-91.

Sun, Y., Clemens, S. C., Morrill, C., Lin, X., Wang, X., & An, Z. (2012). Influence of Atlantic meridional overturning circulation on the East Asian winter monsoon. Nature Geoscience, 5(1), 46-49.

Wang, J., Cui, H., Harbor, J. M., Zheng, L., & Yao, P. (2015). Mid-MIS3 climate inferred from reconstructing the Dalijia Shan ice cap, north-eastern Tibetan Plateau. Journal of Quaternary Science, 30(6), 558-568.

Wang, M., Zong, Y., Zheng, Z., Man, M., Hu, J., & Tian, L. (2018). Utility of brGDGTs as temperature and precipitation proxies in subtropical China. Scientific Reports, 8(1), 1-9.

Wang, Y. J., Cheng, H., Edwards, R. L., An, Z. S., Wu, J. Y., Shen, C. C., & Dorale, J. A. (2001). A high-resolution absolute-dated late Pleistocene monsoon record from Hulu Cave, China. Science, 294(5550), 2345-2348.

Wang, Y. J., Cheng, H., Edwards, R. L., An, Z. S., Wu, J. Y., Shen, C. C., & Dorale, J. A. (2001). A high-resolution absolute-dated late Pleistocene monsoon record from Hulu Cave, China. Science, 294(5550), 2345-2348.

Weijers, Johan WH, Stefan Schouten, Jurgen C. van den Donker, Ellen C. Hopmans, and Jaap S. Sinninghe Damsté. "Environmental controls on bacterial tetraether membrane lipid distribution

in soils." Geochimica et Cosmochimica Acta 71, no. 3 (2007): 703-713.Xiao, W., Xu, Y., Ding, S., Wang,

Xiao, Wenjie, Yunping Xu, Su Ding, Yinghui Wang, Xinyu Zhang, Huan Yang, Guoan Wang, and Juzhi Hou. "Global calibration of a novel, branched GDGT-based soil pH proxy." Organic Geochemistry 89 (2015): 56-60.

Yanai, M., Li, C., & Song, Z. (1992). Seasonal heating of the Tibetan Plateau and its effects on the evolution of the Asian summer monsoon. Journal of the Meteorological Society of Japan. Ser. II, 70(1B), 319-351.